

Two-Dimensional Correlation Gel Permeation Chromatography Study of Octyltriethoxysilane Sol–Gel Polymerization Process

Kenichi Izawa,[†] Toshiaki Ogasawara,[‡] Hideki Masuda,[§]
Hirofumi Okabayashi,^{*,§} and Isao Noda[⊥]

Fuji Silysia Chemical Ltd., Nakatsugawa Technical Center, 1683-1880, Nakagaito, Nasubigawa, Nakatsugawa, Gifu 509-9132, Japan; Tokai Technical Center Foundation, 710, Inokoshi2, Meito-ku, Nagoya, Aichi, 465-0021, Japan; Department of Applied Chemistry, Nagoya Institute of Technology, Gokiso-cho, Showa-ku, Nagoya, Aichi 466-8555, Japan; and The Procter and Gamble Company, 8611 Beckett Road, West Chester, Ohio 45069

Received May 2, 2001

ABSTRACT: A novel analytical method called *two-dimensional correlation gel permeation chromatography* (2D GPC) is introduced. In 2D GPC, generalized two-dimensional (2D) correlation analysis is combined with time-resolved gel permeation chromatography (GPC). This technique can be used effectively, for example, to study intricate details of a polymerization process. In this study, a sol–gel polymerization process of octyltriethoxysilane catalyzed by 1.0 M HCl·H₂O is traced as a function of reaction time using the GPC technique. A set of GPC traces sequentially collected at different sampling points during the polymerization reaction are then converted to two-dimensional correlation maps. It has been found that the 2D GPC maps created by the correlation analysis directly reflect the reaction mechanism in the polymerization process, thus demonstrating the promising potential of this technique.

Introduction

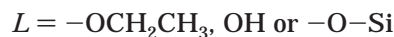
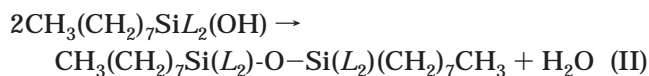
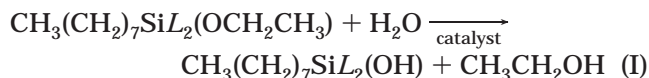
Gel permeation chromatography (GPC) has been well recognized as a useful separation technique based on size exclusion in a liquid chromatographic field. Generally, the main purpose of GPC is an analysis of the molecular weight or distribution of molecular weight of an unknown sample by the size exclusion technique in terms of hydrodynamic volume. The GPC technique is, thus, suitable to detect the composition of solute as a volume distribution, which reflects the molecular structure, aggregation state, and molecular weight.¹ However, the application of time-resolved GPC to investigate a reaction process has not been well recognized yet as a viable analytical technique. The GPC technique has been generally viewed as unsuitable to obtain the time-resolved data. Some limitations of the GPC technique must also be taken into account. For the use of GPC technique, a sample must have a good solubility for an eluent and should not have an interaction with a column used. Moreover, gelation should not occur in the column. It was found that the reaction system of silane coupling agent with *n*-octyl chain can be analyzed effectively by GPC because, in this polymerization process, we can control easily the time for occurrence of macroscopic phase separation by changing the amount of catalysis used. Thus, the phenomenon of the so-called sol–gel transition may be followed in detail by use of the time-resolved GPC profiles.

The two-dimensional (2D) correlation technique^{2–4} has been successfully applied to the analysis of dynamic spectral intensity variations in various molecular spectra, such as IR, Raman, and NIR.^{5–10} It is thought that this technique could also become a powerful tool to examine the fine details of reaction dynamics in polymerization processes observed by time-resolved gel

permeation chromatography. Such a concept, *two-dimensional correlation gel permeation chromatography* (2D GPC), has never been attempted in the past for the study of reaction dynamics. We report here the first example of 2D GPC analysis applied to the study of a sol–gel polymerization process.

In 2D GPC, a series of GPC traces are collected as a function of the sampling time, e.g., reaction time during the course of a polymerization process. The time-resolved GPC traces are then converted to a set of two-dimensional correlation spectra or maps by using a simple mathematical manipulation based on cross-correlation analysis. The resulting 2D GPC maps reveal a lot of useful information not readily observable by conventional GPC methods.

In the present study, we report the 2D correlation analysis of time-resolved GPC profiles to examine the time-dependent behaviors of randomly polymerizing precursors in the octyltriethoxysilane (OTES)–ethanol–1.0 M HCl·H₂O system. In particular, the focus has been placed on the initial 10 min of the reaction process. The reaction may be expressed by the following scheme:



Equation I expresses the hydrolysis reaction process of the silane coupling agent, and eq II is regarded as condensation reaction process during hydrolyzed silane coupling agent monomers and also during oligomer. The same system was investigated previously by using time-resolved SAXS.¹¹ The fractal growth of the OTES polymerization process was followed in the study, and the result showed that the growth process consists of two separate steps: monomer–monomer growth process

[†] Fuji Silysia Chemical Ltd.

[‡] Tokai Technical Center Foundation.

[§] Nagoya Institute of Technology.

[⊥] The Procter and Gamble Company.

* To whom all correspondence should be addressed.

and cluster-cluster growth process. Significantly, the second step, which can be regarded as a transition to build a macroscopic structure, occurs far before macroscopic phase separation. It is therefore very interesting to probe this system by using time-resolved GPC combined with 2D correlation analysis to further elucidate the intricate polymerization process.

The cross-correlation chromatography (so-called CCC) has been used for trace analysis.¹²⁻¹⁵ However, the correlation methods, based on classical statistics, are not able to extract the asynchronous nature of dynamic processes. The concept of generalized 2D correlation, which was introduced by Noda,²⁻⁴ made it possible to analyze systematically such asynchronous characteristics.

Background

The theoretical background of generalized two-dimensional correlation analysis proposed by Noda²⁻⁴ has been applied to various spectroscopic techniques, including IR, Raman, and NIR studies.⁵⁻¹⁰ On the basis of the original concept of 2D spectral analysis, we expand this versatile theory of 2D correlation to GPC elution profiles. In a recent communication,¹⁷ only a very brief description of the 2D GPC concept has been presented. A more detailed description of this powerful technique is now provided.

Dynamic GPC Trace Profiles. Let us consider a time-dependent variation of a GPC trace profile, such as intensity changes of refractive index, or any other physical quantity representing the sample concentration in the eluent conveniently detected for GPC analysis. This time-resolved GPC trace intensity $I(E, t)$, is obtained as a function of not only the chromatographic elution time E but also the sampling time t of the polymerization reaction for each aliquot collected during the period between T_{\min} and T_{\max} . The *dynamic GPC trace intensity* $\tilde{y}(E, t)$ of the time-resolved GPC measurement is given by

$$\tilde{y}(E, t) = \begin{cases} I(E, t) - \bar{I}(E) & \text{for } T_{\min} \leq t \leq T_{\max} \\ 0 & \text{otherwise} \end{cases} \quad (1)$$

where $\bar{I}(E)$ is the *reference GPC trace profile* of the system. In most practical cases, it is customary to set the reference trace $\bar{I}(E)$ to be the time-average of trace profiles over the observation period defined by

$$\bar{I}(E) = \frac{1}{T_{\max} - T_{\min}} \int_{T_{\min}}^{T_{\max}} I(E, t) dt \quad (2)$$

The reference trace could sometimes also be set simply equal to zero; in that case, the dynamic trace is identical to the observed variation of the GPC trace profile. We adopt the conventional form of reference trace defined by eq 2 for our 2D GPC analysis.

Generalized 2D Correlation. The generalized 2D correlation function^{3,4} for time-resolved GPC analysis is formally defined as

$$\Phi(E_1, E_2) + i\Psi(E_1, E_2) = \frac{1}{\pi(T_{\max} - T_{\min})} \int_0^\infty \tilde{Y}_1(\omega) \tilde{Y}_2^*(\omega) d\omega \quad (3)$$

The two orthogonal (i.e., real and imaginary) components of the 2D correlation function, $\Phi(E_1, E_2)$ and $\Psi(E_1, E_2)$, are known respectively as the *synchronous*

and *asynchronous* 2D correlation intensities. The synchronous 2D correlation intensity $\Phi(E_1, E_2)$ represents the overall similarity or coincidental trends between two separate concentration indicator (e.g., refractive index intensity) variations of the GPC trace measured at different elution counts, as the value of sampling (i.e., reaction) time t is scanned from T_{\min} to T_{\max} . The asynchronous 2D correlation intensity $\Psi(E_1, E_2)$, on the other hand, may be regarded as a measure of dissimilarity or out-of-phase character of the GPC trace intensity variations.

The term $\tilde{Y}_1(\omega)$ is the forward Fourier transform of the dynamic trace intensity variations $\tilde{y}(E_1, t)$ observed at some given elution count E_1 with respect to the sampling time t . It is given by

$$\tilde{Y}_1(\omega) = \int_{-\infty}^\infty \tilde{y}(E_1, t) e^{-i\omega t} dt \quad (4)$$

According to eq 1, the above Fourier integration of the dynamic spectrum is actually bound by the finite interval between T_{\min} and T_{\max} . The Fourier frequency ω represents the individual frequency component of the variation of $\tilde{y}(E_1, t)$ traced along the sampling time t . Likewise, the conjugate of the Fourier transform $\tilde{Y}_2^*(\omega)$ of the refractive index intensity variation $\tilde{y}(E_2, t)$ observed at elution time E_2 is given by

$$\tilde{Y}_2^*(\omega) = \int_{-\infty}^\infty \tilde{y}(E_2, t) e^{+i\omega t} dt \quad (5)$$

Once the appropriate Fourier transformation of the dynamic trace $\tilde{y}(E, t)$ defined in the form of eq 1 is carried out with respect to the reaction sampling time t , eq 3 will directly yield the synchronous and asynchronous correlation spectra, $\Phi(E_1, E_2)$ and $\Psi(E_1, E_2)$. The basic properties of generalized 2D correlation spectra are provided in detail elsewhere.^{3,4} Here, some specific features applicable to the interpretation of 2D GPC spectra are presented.

Synchronous 2D GPC Spectrum. The intensity of a synchronous 2D GPC correlation spectrum $\Phi(E_1, E_2)$ represents the simultaneous or coincidental changes of GPC trace intensity variations measured at elution times E_1 and E_2 during the observation interval between T_{\min} and T_{\max} of the reaction sampling time t . A synchronous spectrum is a symmetric spectrum with respect to the diagonal line corresponding to coordinates $E_1 = E_2$. Correlation peaks appear at both diagonal and off-diagonal positions.

The intensity of peaks located at diagonal positions mathematically corresponds to the autocorrelation function of GPC trace intensity variations observed during an observation interval between T_{\min} and T_{\max} . The diagonal peaks are therefore referred to as *autopeaks*, and the slice trace of a synchronous 2D spectrum along the diagonal is called the *autopower spectrum*. The magnitude of an autopeak intensity, which is always positive, represents the overall extent of GPC trace intensity variation observed at the specific elution count E . Thus, any regions of a GPC trace which change the trace intensity to a great extent under a given reaction process will show strong autopeaks, while those remaining near constant develop little or no autopeaks. In other words, an autopeak represents the overall susceptibility of the corresponding GPC profile to change in the trace intensity as the polymerization reaction is progressing.

Cross-peaks located at the off-diagonal positions of a synchronous 2D GPC spectrum represent simultaneous

or coincidental changes, either increase or decrease, of GPC trace intensities observed at two different elution counts E_1 and E_2 . Such a synchronized change, in turn, suggests the possible existence of a coupled or related origin of the GPC trace intensity variations. It is often useful to construct a *correlation square* joining the pair of cross-peaks located at opposite sides of a diagonal line drawn through the corresponding autopeaks to show the existence of coherent variation of GPC trace intensity at these spectral variables.

While the sign of autopeaks is always positive, the sign of cross-peaks can be either positive or negative. The sign of synchronous cross-peaks becomes positive if the GPC trace intensities at the two elution times corresponding to the coordinates of the cross-peak are either increasing or decreasing together as functions of the sampling time t during the observation interval. On the other hand, the negative sign of cross-peaks indicates that one of the GPC trace intensities is increasing while the other is decreasing.

Asynchronous 2D GPC Spectrum. The intensity of an asynchronous spectrum represents sequential or successive changes of GPC trace intensities measured at E_1 and E_2 . Unlike a synchronous spectrum, an asynchronous spectrum is antisymmetric with respect to the diagonal line. The asynchronous spectrum has no autopeaks and consists exclusively of cross-peaks located at off-diagonal positions. By extending lines from the spectral coordinates of cross-peaks to corresponding diagonal positions, one can construct asynchronous correlation squares.

An asynchronous cross-peak develops only if the intensities of two GPC trace features change out of phase with each other, i.e., delayed or accelerated with respect to sampling time. This feature is especially useful in differentiating overlapped bands arising from GPC profiles of different origins. For example, different GPC trace intensity contributions from individual components of a complex mixture may be effectively discriminated. Even if bands are located close to each other, as long as the signatures or the pattern of sequential variations of trace intensities are substantially different, asynchronous cross-peaks will develop between their GPC trace coordinates.

The sign of asynchronous cross-peaks can be either negative or positive. The sign of an asynchronous cross-peak becomes positive if the intensity change at E_1 occurs predominantly before E_2 in the sequential order of sampling time t . It becomes negative, on the other hand, if the change occurs after E_2 . This rule, however, is reversed if $\Phi(E_1, E_2) < 0$. These simple but useful rules are all based on the well-established theory of 2D correlation analysis.^{3,4}

Experimental Section

Materials. Octyltriethoxysilane (OTES) was purchased from Fluka Chemical Ltd. and was used without further purification. An OTES–ethanol–1.0 M HCl·H₂O (1:1:0.4 weight ratio) system was used as an acid-catalyzed reaction mixture at 25 °C. In this study, the initial 10 min period was focused to follow a rapid polymerization process.

Time-Resolved Gel Permeation Chromatography Measurements. Gel permeation chromatography (GPC) measurements were carried out by using a SHIMADZU high-performance liquid chromatography system, which consists of a column oven CTO-10Avp equipped with Asahipack GF-310HQ column (300 (L) × 7.6 (φ) mm) operated at 30 °C, a high pressure solvent delivery pump LC-10Advp, a DGU-14A

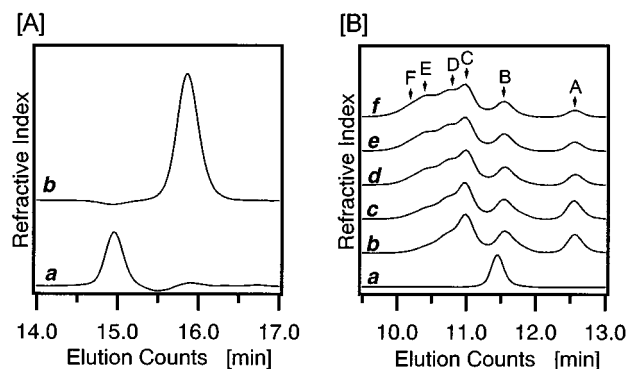


Figure 1. (A) GPC elution profiles of APTES (a) and APTHS (b) and (B) time-resolved GPC elution profiles of OTES (a, monomer ($t = 0$); b, 60 s; c, 180 s; d, 300 s; e, 420 s; f, 540 s).

degasser, and refractive index (RI) detector RID-10A. Tetrahydrofuran was used as the eluent at a flow rate of 0.6 mL/min. The system was calibrated with polystyrene standards. Time-resolved GPC profiles were obtained by the following method. Aliquots of 0.002 mL were sampled from the reaction mixture of the OTES–ethanol–HCl·H₂O system every 60 s in the time range 60–540 s. Each aliquot was quickly diluted by 1 mL of THF chilled at 273 K to quench the reaction. Thus, 10 time-sliced samples reflecting the time-dependent compositional changes were obtained. For each THF-diluted sample solution, normal GPC analysis was conducted.

In the GPC profiles, the S/N ratios of the elution peaks and of the baseline were checked to prevent the error in the interpretation of the 2D correlation maps. The average S/N ratios were 90–95.

2D Correlation Analysis. Synchronous and asynchronous 2D GPC correlation spectra were calculated from the time-resolved GPC elution profiles using the generalized 2D correlation procedure described by eqs 1–3. The computation was carried out using the 2D OGAIZA software based on the algorithm incorporating eqs 1–3.

Results and Discussion

Time-Resolved GPC Elution Profiles of OTES

Polymerization Process. The GPC elution profiles of (aminopropyl)triethoxysilane (APTES) and (aminopropyl)triethoxysilane (APTHS) are shown in Figure 1A. The elution times of APTES and APTHS are 14.96 and 15.85 min, respectively, and reflect the difference in the quantity of ethoxy moieties, which remains unreacted. This result indicates that the ethoxy group is bulky enough to distinguish the extent of hydrolysis reaction using the refractive index method. For the peak assignment of OTES–ethanol system, the elution pattern of aminopropylsilane was used to examine the difference in the extent of hydrolysis reaction in each elution profile.

The GPC profiles, which were obtained during the polymerization process of octyltriethoxysilane (OTES) catalyzed with 1.0 M HCl·H₂O, are shown in Figure 1B. The OTES monomer (profile a) has only one elution band at 11.5 min, but after 60 s of reaction time (profile b), three predominant elution bands appear at 11.0, 11.6, and 12.6 min. The band A at 12.6 min can be identified as octyltriethoxysilane (OTHS), since it should provide the same pattern as the case of aminopropyltriethoxysilane. We may assume that the reaction of hydrolysis mainly occurs during the initial 60 s period of reaction time. The assignment of each band listed in Table 1 is based on the elution behaviors of APTES and APTHS as mentioned above. The band B at 11.6 min may be considered as a broadened band consisting of

Table 1. Elution Peak Assignments in Time-Resolved GPC Profile of the OTES System

elution count [min]	band no.	assignment
12.6	A	trihydrolyzed OTES
11.6	B	broadened OTES
11.0	C	polymer I
10.8	D	polymer II
10.4	E	polymer III
10.2	F	polymer IV

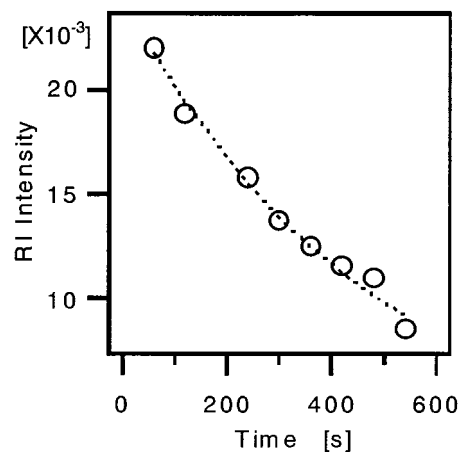
OTES and partially hydrolyzed OTES (ph-OTES, i.e., a mixture of monohydroxysilane (OMHS) and dihydroxysilane (ODHS)). The broad band at 11.0 min and other bands with lower elution counts (bands C–F) may arise from polymeric precursors such as dimer, trimer, and larger oligomers. These profiles clearly reflect the process of the OTHS condensation reaction.

Figure 2 shows the reaction time dependence of GPC trace intensity of band A. We may regard the band A as an elution peak of single substance of fully hydrolyzed monomeric precursor to build three-dimensional siloxane bonds. If all monomeric molecules are hydrolyzed immediately after the start of the reaction, and no substantial condensation reaction occurs at this stage, the band A substance (that is, OTHS) should be consumed to form a new polymeric precursor. Thus, the variation in the profile of the band should reflect the kinetics of the polymerization process. A kinetic analysis for the time-dependent GPC trace intensity data was carried out by assuming the first-order reaction. The rate constant thus obtained is $k = 2.11 \times 10^{-3} \text{ s}^{-1}$, which is faster compared to the rate constant ($k = 2.35 \times 10^{-4} \text{ s}^{-1}$) obtained from the NIR data for the condensation reaction based on the time dependence of water production of perfluorotrimethoxysilane.¹⁸ The difference in the reaction rate must be caused by the different properties of hydroalkyl chain and fluoroalkyl chain.

Two-Dimensional GPC (2D GPC) Analysis of OTES Polymerization Process. To achieve better understanding of the complex polymerization process, the *two-dimensional GPC* (2D GPC) analysis was carried out using these time-resolved GPC profiles. The synchronous and asynchronous 2D GPC correlation maps obtained from the time-resolved GPC profiles in the initial stage (0–540 s) are shown in parts A and B of Figure 3, respectively. The peak locations and the orders are listed in Table 2.

In the synchronous 2D correlation map (Figure 3A), the five major autopeaks were observed at the elution times of 12.6, 11.6, 11.4, 11.0, and 10.4. The synchronous correlation map consists of numerous independent cross-peaks, and correlation squares can be constructed with all peaks. We should note the band B consisting of two different peaks (OTES monomer (B_2) and ph-OTES (B_1)), which provide two cross-peaks (11.4 and 11.6). Since the peak B_2 comes from monomer (OTES), this peak decreases in intensity as the reaction proceeds, bringing about the negative cross-peak at (11.4, 11.0). Conversely, the band B_1 (ph-OTES) increases in intensity, as the monomer molecules are partially hydrolyzed, resulting in the positive peak (11.6, 11.0). Thus, the negative correlation peaks arise from the coordinated decrease in B_2 peak and simultaneous increase in the B_1 peak.

The asynchronous correlation map (Figure 3B) directly provides the order of events.^{2,3} The relationship among peaks B_1 , B_2 , and A may provide the order of the hydrolysis process for OTES (through ph-OTES to

**Figure 2.** Reaction time dependence of refractive index (RI) intensity at GPC elution time of 12.56 min (band A).**Table 2. Sign of Correlation Peaks in Synchronous and Asynchronous Diagram**

(E_1, E_2)	sign		order ^a
	Φ syn int	Ψ asyn int	
(12.6, 11.6)	+	+	$E_1 \rightarrow E_2$
(12.6, 11.4)	–	–	$E_2 \rightarrow E_1$
(12.6, 11.0)	+	+	$E_1 \rightarrow E_2$
(11.6, 11.4)	–	–	$E_2 \rightarrow E_1$
(11.6, 11.0)	+	+	$E_1 \rightarrow E_2$
(11.4, 11.0)	–	–	$E_2 \rightarrow E_1$
(11.4, 10.7)	–	–	$E_2 \rightarrow E_1$
(11.4, 10.4)	–	–	$E_2 \rightarrow E_1$
(11.7, 10.7)	+	+	$E_1 \rightarrow E_2$
(11.0, 10.4)	+	+	$E_1 \rightarrow E_2$
(10.7, 10.4)	+	+	$E_1 \rightarrow E_2$

^a $E_x \rightarrow E_y$: the event of E_x occurs before that of E_y .

the final product OTHS). When peak B_1 is compared to B_2 , the asynchronous cross-peak sign is negative and the synchronous cross-peak sign is also negative. According to the rules established for interpreting the signs of asynchronous cross-peaks, the decrease in band B_2 occurs first, and then an increase in band B_1 follows later. In other words, the hydrolysis reaction of OTES occurs at first, and then the production of ph-OTES follows. The relationship between bands B_1 and A as well as that between bands B_2 and A can be deduced as follows. The change of band A occurs first, and then the band B_1 change follows. Likewise, the change of band B_2 happens first, and then the band A is changed (see Table 2). These findings indicate that the consumption of monomer may be connected with the production of ph-OTES and OTHS. Judging from the asynchronous map, the reducing rate of OTHS is faster than the production of ph-OTES, implying that the condensation reaction happens faster than the hydrolysis reaction does in this stage.

We have examined the time-resolved near-IR spectra of the same reaction system in the initial stage. A kinetic analysis of the increased absorbance data of the 5160 cm^{-1} band (the combination mode between the H_2O deformation and H_2O asymmetric stretch modes) and of the 4817 cm^{-1} band (the combination mode between the alcohol OH stretch and bend mode) was carried out by assuming the first-order reaction. The values of the rate constants, thus obtained, are $k = 4.31 \times 10^{-2} \text{ s}^{-1}$ for the water band and $k = 2.27 \times 10^{-2} \text{ s}^{-1}$ for the ethanol band, indicating that the production of water as a consequence of condensation reaction is

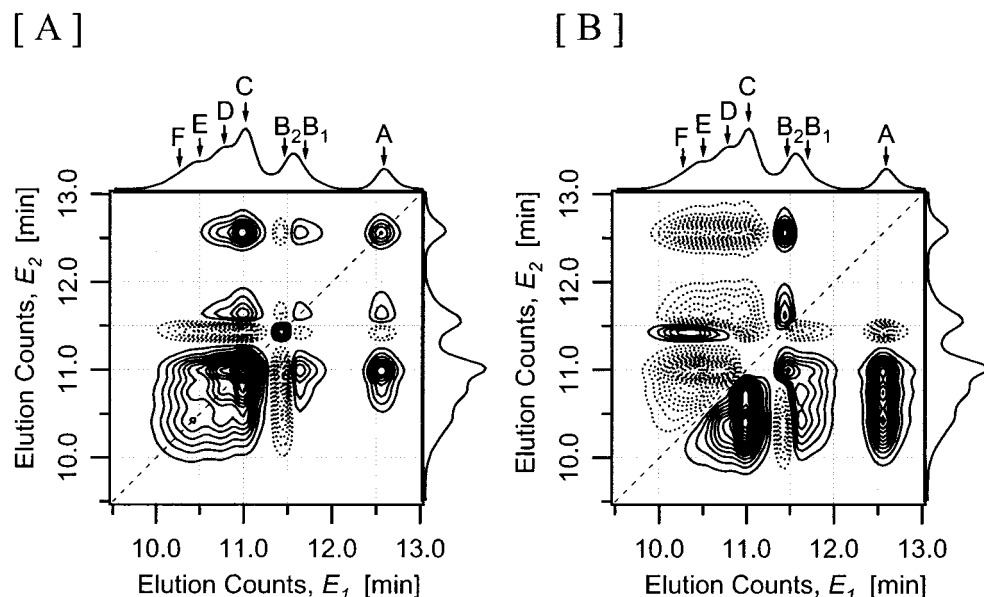
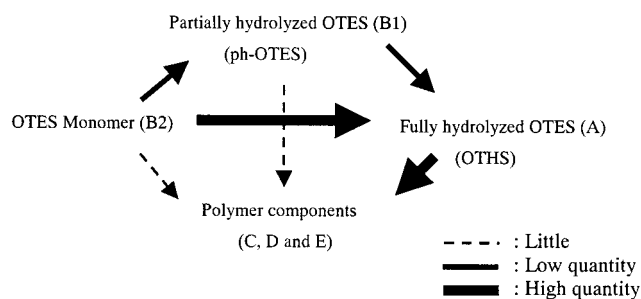


Figure 3. (A) Synchronous and (B) asynchronous correlation spectrum of the OTES-ethanol-1.0 M HCl-H₂O system obtained for the initial 60 s. Solid line indicates a positive peak, and broken line indicates a negative peak.

Scheme 1. Schematic Polymerization Process of OTES



faster compared with that of ethanol by the hydrolysis reaction. This NIR data strongly support the result obtained from the asynchronous map described above.

For other bands, C, D, and E, we may conclude that these band compositions may be consumed after the consumption of OTHS and ph-OTES, except the relationship between OTES (B₂) and polymeric band D and E. The relationship of these peaks implies that the production of polymeric components (D and E) occurs at first, and then OTES (B₂) is consumed. From the relationship among C, D, and E, we may assume that component C is produced at first, and then the production of D component follows. Finally, production of E component may occur.

Thus, it is evident that the order of events for all elution peaks can be determined from only one asynchronous spectrum. This fact, which comes from characteristics of the asynchronous correlation spectrum, cannot be obtained by the conventional GPC method.

The sequence of intricate reaction steps deduced from the 2D GPC correlation analysis may be summarized as shown in Scheme 1.

Conclusions

The generalized 2D correlation approach is extended for the first time to the analysis of time-resolved GPC measurement, leading to the development of the concept of 2D GPC correlation analysis. When applied to the study of OTES sol-gel polymerization, 2D GPC provides a detailed description of the polymerization process in

terms of the relationship between monomeric and polymeric precursors. OTES monomers are hydrolyzed within the first 60 s to produce fully hydrolyzed monomers, and fully hydrolyzed monomers are mainly consumed to produce polymeric precursors. The polymeric precursors, however, is formed not only by fully hydrolyzed monomers but also by OTES monomers and partially hydrolyzed monomers. The 2D GPC correlation analysis provides direct information about the time-dependent relationship among these precursors during the reaction process. The result clearly demonstrates the promising potential of this newly introduced analytical technique.

References and Notes

- (1) *Strategies in Size Exclusion Chromatography*; Potschka, M., Dubin, P. L., Eds.; ACS Symposium Series 653; American Chemical Society: Washington, DC, 1996.
- (2) Noda, I. *Appl. Spectrosc.* **1990**, *44*, 550–561.
- (3) Noda, I. *Appl. Spectrosc.* **1993**, *47*, 1329–1336.
- (4) Noda, I.; Dowrey, A. E.; Marcott, C.; Story, G. M.; Ozaki, Y. *Appl. Spectrosc.* **2000**, *54*, 236A–248A.
- (5) Noda, I.; Liu, Y.; Ozaki, Y.; Czarniecki, M. *J. Phys. Chem.* **1995**, *99*, 3068–3073.
- (6) Noda, I.; Liu, Y.; Ozaki, Y. *J. Phys. Chem.* **1996**, *100*, 8674–8680.
- (7) Ozaki, Y.; Liu, Y.; Noda, I. *Macromolecules* **1997**, *30*, 2391–2399.
- (8) Ren, Y.; Shimoyama, M.; Ninomiya, T.; Matsukawa, K.; Inoue, H.; Noda, I.; Ozaki, Y. *J. Phys. Chem. B* **1999**, *103*, 6475–6483.
- (9) Sefara, N. L.; Magtoto, N. P.; Richardson, H. H. *Appl. Spectrosc.* **1997**, *51*, 536–540.
- (10) Ogasawara, T.; Nara, A.; Okabayashi, H.; Nishio, E.; O'Connor, C. J. *Colloid Polym. Sci.* **2000**, *278*, 1070–1084.
- (11) Ogasawara, T.; Izawa, K.; Hattori, N.; Okabayashi, H.; O'Connor, C. J. *Colloid Polym. Sci.* **2000**, *278*, 293–300.
- (12) Smit, H. C. *Chromatographia* **1970**, *3*, 515–518.
- (13) Phillips, J. B.; Burke, M. F. *J. Chromatogr. Sci.* **1976**, *4*, 495–497.
- (14) Kaljurand, M.; Küllik, E. *J. Chromatogr.* **1979**, *186*, 145–158.
- (15) Annino, R. *ACS Symp. Ser.* **1985**, *284*, Chapter 6.
- (16) Izawa, K.; Ogasawara, T.; Masuda, H.; Okabayashi, H.; Noda, I., submitted for publication.
- (17) Ogasawara, T.; Nara, A.; Okabayashi, H.; Nishio, E.; O'Connor, C. J. *Colloid Polym. Sci.* **2000**, *278*, 946–953.